一般社団法人　電子情報通信学会
THE INSTITUTE OF ELECTRONICS,
INFORMATION AND COMMUNICATION ENGINEERS

信学技報
IEICE Technical Report
RCS2016-182(2016-10)

2-Step Signal Detection for Blind Time-Domain Selected Mapping

Amnart Boonkajay † and Fumiyuki Adachi ‡

† ‡ Research Organization of Electrical Communication (ROEC), Tohoku University
2-1-1 Katahira, Aoba-ku, Sendai, Miyagi, 980-8577 Japan
E-mail: † amnart@riec.tohoku.ac.jp ‡ adachi@ecei.tohoku.ac.jp

Abstract Single-carrier signal transmission with frequency-domain receive equalization and space-time block coded transmit diversity (called SC-FDE/STTD) is a promising uplink broadband transmission. However, the peak-to-average power ratio (PAPR) of SC-FDE/STTD signal increases although SC signal has lower PAPR than orthogonal frequency division multiplexing (OFDM) signal. The blind time-domain selected mapping (blind TD-SLM) can reduce the PAPR of SC-FDE/STTD without side-information transmission. In our previous works, maximum likelihood (ML) estimation was applied to find the de-mapping phase rotation sequence which gives the lowest Euclidean distance between the de-mapped signal and the original data modulated signal constellation among all possible sequences, resulting in very high computational complexity. In this paper, we introduce a novel low-complexity 2-step estimation suitable for blind TD-SLM. In the first step, the phase rotation sequence achieving the lowest Euclidean distance is searched by using the Viterbi algorithm. In the second step, verification and correction are carried out to choose a phase rotation sequence stored in the codebook, which has the lowest Hamming distance from the estimated sequence in the first step. It is confirmed by simulation that our proposed 2-step estimation achieves similar BER performance to ML estimation while requiring much less computational complexity.

Keyword Single-carrier (SC) transmission, space-time transmit diversity (STTD), peak-to-average power ratio (PAPR), selective mapping (SLM)

1. Introduction

Single-carrier (SC) signal transmission with frequency-domain receive equalization (FDE) [1] and space-time block coded transmit diversity (STTD) [2] is very attractive for uplink transmission. It is called SC-FDE/STTD in this paper. It obtains high diversity gain [3], while its waveform has low peak-to-average power ratio (PAPR). The low-PAPR transmit waveform leads to low power consumption in power amplifier (PA), resulting in longer battery life in a user equipment (UE).

If the ideal rectangular frequency-domain band-limiting transmit filter is applied to SC signal (this is equivalent to discrete Fourier transform (DFT)-precoded orthogonal frequency division multiplexing (OFDM) [4]), the PAPR in SC signal increases even though it still remains lower than that of OFDM signal [5]. Recently, we have introduced a PAPR reduction technique for filtered SC signal based on phase rotation called selected mapping (SLM) [6]. The proposed SLM in [6] is simple and is able to reduce the PAPR effectively but at the cost of overhead (side-information notifying which phase rotation sequence is used). A blind SLM technique for filtered SC signal, in which the receiver estimates the selected phase rotation sequence without requiring side-information, was proposed in [7]. An application of blind SLM to SC-FDE/STTD clarified [8] that low-PAPR signal is achieved even in multi-antenna transmission and there is no significant bit-error rate (BER) degradation.

Phase rotation sequence estimation for blind SLM in [7-8] employs maximum likelihood (ML) estimation. ML estimation searches the mapping sequence used at the transmitter by computing the Euclidean distance between the de-mapped signal and original data-modulated signal constellation (before mapping at the transmitter) among all possible sequences. The de-mapping sequence which gives the lowest Euclidean distance is chosen for succeeding data demodulation. However, ML estimation requires high computational complexity, and hence is impractical when the number of sequences is large.

To achieve low-PAPR transmission with low-complexity receiver, we introduce a novel 2-step phase rotation sequence estimation for blind TD-SLM. The proposed estimation technique can be briefly described as follows. In the first step, the phase rotation sequence giving the lowest Euclidean distance is searched by using Viterbi algorithm [9]. In the second step, verification and correction are carried out to choose a phase rotation sequence which is stored in the codebook and has the lowest Hamming distance from the estimated sequence obtained from the first step. Computer simulation results are provided to show that the proposed 2-step estimation achieves similar BER compared to the ML estimation but with much less computational complexity. As its contribution, we can further increase the number of phase rotation sequences for achieving very low-PAPR signal.

2. Transmitter system model

The transmitter of SC-FDE/STTD with blind SLM is shown in Fig. 1. For simplicity, point-to-point block transmission using N_t transmit antennas and N_r receive

antennas is assumed in this paper. The first N_s subcarriers are selected from N_c available subcarriers to contain data. The transmit signal and processing techniques are represented by row vector and matrices, respectively.

Let $\mathbf{d}=[\mathbf{d}_0,\mathbf{d}_1,...,\mathbf{d}_{J-1}]^T$, j=0~J−1 denote J blocks of N_s-length data-modulated transmit vector where $\mathbf{d}_j=[d_j(0),d_j(1),\ldots,d_j(N_s-1)]^T$. The transmit blocks are then phase rotated by the selected phase rotation matrix $\mathbf{P}_{\hat{m}}=diag[\mathbf{P}_{\hat{m}_0},...,\mathbf{P}_{\hat{m}_j},...\mathbf{P}_{\hat{m}_{J-1}}]$, yielding the phase-rotated time-domain signal $\mathbf{x}=\mathbf{P}_{\hat{m}_j}\mathbf{d}$, where $\mathbf{x}=[\mathbf{x}_0,\mathbf{x}_1,...,\mathbf{x}_{J-1}]^T$ and j=0~J−1. The phase rotation sequence $\mathbf{P}_{\hat{m}_j}$ is an $N_s\times N_s$ diagonal matrix which minimize the PAPR of $\mathbf{d}_j$. The selection criterion can be expressed as [7]

$$\mathbf{P}_{\hat{m}_j}=\arg\min_{m=0,1,...,M-1}(\mathrm{PAPR}(\mathbf{F}_{N_c}^H\mathbf{H}_T\mathbf{F}_{N_s}\mathbf{P}_m\mathbf{d}_j)), \tag{1}$$

where $\mathbf{F}_{N_c}$ and $\mathbf{F}_{N_c}^H$ represents the DFT and inverse DFT (IDFT), respectively. M represents the number of available phase rotation sequences. PAPR of a particular N_c-length time-domain transmit block $\mathbf{s}=[s(0),s(1),\ldots,s(N_c-1)]^T$ is described by

$$\mathrm{PAPR}(\mathbf{s})=\frac{\max\{|s(n)|^2,n=0,\frac{1}{V},\frac{2}{V},...,N_c-1\}}{\frac{1}{N_c}\sum_{n=0}^{N_c-1}|s(n)|^2}, \tag{2}$$

where V is oversampling factor. Transmit filtering matrix $\mathbf{H}_T=diag[H_T(0),...,H_T(N_c-1)]$ is assumed to be an ideal rectangular filter, i.e. $H_T(k)$=1 if $k<N_s$ and $H_T(k)$=0 elsewhere.

Table 1 Relationship of N_t, J, Q and STBC coding rate.

N_t	J	Q	$R_{\mathrm{STBC}}=J/Q$
1	1	1	1
2	2	2	1
3	3	4	3/4
4	3	4	3/4

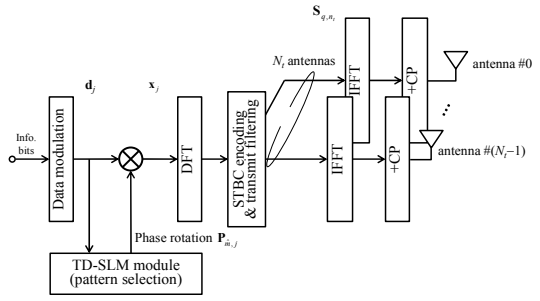

Fig. 1 Transmitter.

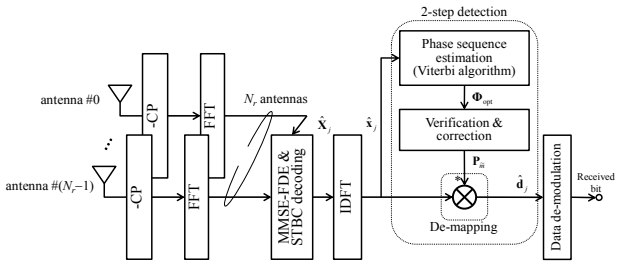

Fig. 2 Receiver.

Next, the j-th transmit block $\mathbf{x}_j$ is transformed into frequency domain by N_s-point DFT, yielding the j-th block of frequency signal $\mathbf{X}_j=[X_j(0),X_j(1),...,X_j(N_s-1)]^T$ as $\mathbf{X}_j=\mathbf{F}_{N_s}\mathbf{x}_j$, where $\mathbf{F}_{N_s}$ is shown by defining $i=\sqrt{-1}$ as

$$\mathbf{F}_{N_s}=\frac{1}{\sqrt{N_s}}\begin{bmatrix}1 & 1 & \cdots & 1\\ 1 & e^{\frac{-i2\pi(1)(1)}{N_s}} & \cdots & e^{\frac{-i2\pi(1)(N_s-1)}{N_s}}\\ \vdots & \vdots & \ddots & \vdots\\ 1 & e^{\frac{-i2\pi(N_s-1)(1)}{N_s}} & \cdots & e^{\frac{-i2\pi(N_s-1)(N_s-1)}{N_s}}\end{bmatrix}, \tag{3}$$

After that, J blocks of frequency-domain signal $\mathbf{X}_j$ are encoded by orthogonal STBC [2], then obtaining N_t streams of Q blocks $\mathbf{S}_{N_t}=[\mathbf{S}_0,...,\mathbf{S}_q,...,\mathbf{S}_{Q-1}]$ where $\mathbf{S}_q=[\mathbf{S}_{q,0},...,\mathbf{S}_{q,n_t},...,\mathbf{S}_{q,N_t-1}]^T$, $\mathbf{S}_{q,n_t}=[S_{q,n_t}(0),...,S_{q,n_t}(N_s-1)]^T$. The encoded blocks $\mathbf{S}_{N_t}$ is expressed by [10]

$$\mathbf{S}_{N_t}=\begin{cases}\mathbf{X}_0 & \text{if } N_t=1,\\ \frac{1}{\sqrt{2}}\begin{bmatrix}\mathbf{X}_0 & -\mathbf{X}_1^*\\ \mathbf{X}_1 & \mathbf{X}_0^*\end{bmatrix} & \text{if } N_t=2,\\ \frac{1}{\sqrt{3}}\begin{bmatrix}\mathbf{X}_0 & -\mathbf{X}_1^* & -\mathbf{X}_2^* & \mathbf{0}\\ \mathbf{X}_1 & \mathbf{X}_0^* & \mathbf{0} & -\mathbf{X}_2^*\\ \mathbf{X}_2 & \mathbf{0} & \mathbf{X}_0^* & \mathbf{X}_1^*\end{bmatrix} & \text{if } N_t=3,\\ \frac{1}{\sqrt{4}}\begin{bmatrix}\mathbf{X}_0 & -\mathbf{X}_1^* & -\mathbf{X}_2^* & \mathbf{0}\\ \mathbf{X}_1 & \mathbf{X}_0^* & \mathbf{0} & -\mathbf{X}_2^*\\ \mathbf{X}_2 & \mathbf{0} & \mathbf{X}_0^* & \mathbf{X}_1^*\\ \mathbf{0} & \mathbf{X}_2 & -\mathbf{X}_1 & \mathbf{X}_0\end{bmatrix} & \text{if } N_t=4,\end{cases} \tag{4}$$

In addition, the relationship between J and Q, and the corresponding coding rate $R_{\mathrm{STBC}}=J/Q$, is shown in Table 1.

After that, $\mathbf{S}_{q,n_t}$ is zero-padded and is transformed back into time domain by N_c-point IDFT, yielding the q-th time-domain transmit block at the n_t-th antenna $\mathbf{s}_{q,n_t}=\mathbf{F}_{N_c}^H\mathbf{S}_{q,n_t}$. IDFT can be changed to inverse fast Fourier transform (IFFT) if N_c is a power of 2. Finally, the last N_g samples of transmit block are copied as a cyclic prefix (CP) and inserted into the guard interval (GI), then a CP-inserted signal block of N_g+N_c samples is transmitted.

3. Receiver system model

The receiver of SC-FDE/STTD using blind SLM is illustrated by Fig. 2. It can be seen that the receiver consists of two main processes; joint FDE based on minimum mean-square error (MMSE-FDE) and STTD decoding, and 2-step phase sequence estimation.

3.1. Joint MMSE-FDE and STTD decoding

The wireless channel is assumed to be a symbol-spaced L-path frequency-selective block Rayleigh fading channel, where its impulse response between the n_t-th transmit antenna and the n_r-th receive antenna is given by

$$h_{n_r,n_t}(\tau)=\sum_{l=0}^{L-1}h_{n_r,n_t,l}\delta(\tau-\tau_{n_r,n_t,l}), \tag{5}$$

where $h_{n_r,n_t,l}$ and $\tau_{n_r,n_t,l}$ are complex-valued path gain and time delay of the l-th path, respectively. In addition,

$h_{n_r,n_t,l}$ is assumed to be the same for Q encoded block in this paper for simplicity. The q-th block received signal at the n_r-th antenna $\mathbf{r}_{q,n_r} = [r_{q,n_r}(0), r_{q,n_r}(1), ..., r_{q,n_r}(N_c-1)]^T$ can be expressed by

$$r_{q,n_r}(t) = \sqrt{\frac{2E_s}{T_s}} \sum_{n_t=0}^{N_t-1} \sum_{l=0}^{L-1} h_{n_r,n_t,l} s_{q,n_t}(t-\tau_{n_r,n_t,l}) + z_{q,n_r}(t), \qquad (6)$$

where $z_{q,n_r}(t)$ is an additive white Gaussian noise (AWGN) having zero mean and the variance of $2N_0/T_s$ with T_s is symbol duration and N_0 being the one-sided noise power spectrum density. Note that the path-loss and shadowing-loss are neglected. After CP removal, $r_{q,n_r}(t)$ is transformed into frequency domain by N_c-point DFT and then applying frequency de-mapping for extracting N_s frequency components. The frequency-domain received signal at the n_r-th antenna and the q-th timeslot $\mathbf{R}_{q,n_r} = [R_{q,n_r}(0), ..., R_{q,n_r}(N_s-1)]^T$ can be expressed by

$$R_{q,n_r}(k) = \sqrt{\frac{2E_s}{T_s}} \sum_{n_t=0}^{N_t-1} H_{n_r,n_t}(k) S_{q,n_t}(k) + Z_{q,n_r}(k), \qquad (7)$$

where the frequency-domain channel response and noise are given by

$$H_{n_r,n_t}(k) = \sum_{l=0}^{L-1} h_{n_r,n_t,l} \exp(-i2\pi k \tau_{n_r,n_t,l} / N_c), \qquad (8a)$$

$$Z_{q,n_r}(k) = \frac{1}{N_c} \sum_{t=0}^{N_c-1} z_{q,n_r}(n) \exp(-i2\pi k t / N_c). \qquad (8b)$$

FDE based on minimum mean-square error criterion (MMSE-FDE) is employed, yielding the equalized signal as $\hat{\mathbf{R}}_{(N_t\times Q)} = \mathbf{W}^H_{(N_t\times N_r)} \mathbf{R}_{(N_r\times Q)}$, where $\mathbf{W} = [\mathbf{W}_0, ..., \mathbf{W}_{n_r}, ..., \mathbf{W}_{N_r-1}]^T$ and $\mathbf{W}_{n_r} = [\mathbf{W}_{n_r,0}, ..., \mathbf{W}_{n_r,n_t}, ..., \mathbf{W}_{n_r,N_t-1}]^T$ represents the MMSE-FDE weight matrix. The FDE weight at the k-th frequency index is expressed by

$$W_{n_r,n_t}(k) = \frac{H_{n_r,n_t}(k)}{\left(\sum_{n_r=0}^{N_r-1} \sum_{n_t=0}^{N_t-1} |H_{n_r,n_t}(k)|^2\right) + (E_s/N_0)^{-1}}. \qquad (9)$$

After that, STTD decoding is carried out in order to achieve spatial diversity gain. The frequency-domain decoded vector $\hat{\mathbf{X}}_j$, j=0~J–1 is obtained by the following STTD decoders [10]

$$\hat{\mathbf{X}}_{N_t} = \begin{cases} \hat{\mathbf{R}}_{0,0} & \text{if } N_t = 1, \\ \begin{bmatrix} \hat{\mathbf{X}}_0 \\ \hat{\mathbf{X}}_1 \end{bmatrix} = \begin{bmatrix} \hat{\mathbf{R}}_{0,0} + \hat{\mathbf{R}}^*_{1,1} \\ \hat{\mathbf{R}}_{0,1} - \hat{\mathbf{R}}^*_{1,0} \end{bmatrix} & \text{if } N_t = 2, \\ \begin{bmatrix} \hat{\mathbf{X}}_0 \\ \hat{\mathbf{X}}_1 \\ \hat{\mathbf{X}}_2 \end{bmatrix} = \begin{bmatrix} \hat{\mathbf{R}}_{0,0} + \hat{\mathbf{R}}^*_{1,1} + \hat{\mathbf{R}}^*_{2,2} \\ \hat{\mathbf{R}}_{0,1} - \hat{\mathbf{R}}^*_{1,0} + \hat{\mathbf{R}}^*_{3,2} \\ \hat{\mathbf{R}}_{0,2} - \hat{\mathbf{R}}^*_{2,0} - \hat{\mathbf{R}}^*_{3,1} \end{bmatrix} & \text{if } N_t = 3, \\ \begin{bmatrix} \hat{\mathbf{X}}_0 \\ \hat{\mathbf{X}}_1 \\ \hat{\mathbf{X}}_2 \end{bmatrix} = \begin{bmatrix} \hat{\mathbf{R}}_{0,0} + \hat{\mathbf{R}}^*_{1,1} + \hat{\mathbf{R}}^*_{2,2} + \hat{\mathbf{R}}_{3,3} \\ \hat{\mathbf{R}}_{0,1} - \hat{\mathbf{R}}^*_{1,0} - \hat{\mathbf{R}}_{2,3} + \hat{\mathbf{R}}^*_{3,2} \\ \hat{\mathbf{R}}_{0,2} + \hat{\mathbf{R}}_{1,3} - \hat{\mathbf{R}}^*_{2,0} - \hat{\mathbf{R}}^*_{3,1} \end{bmatrix} & \text{if } N_t = 4. \end{cases} \qquad (10)$$

After STTD decoding, J blocks of the frequency-domain signal are then transformed back into time domain by N_s-point IDFT, yielding the received vector before de-mapping $\hat{\mathbf{x}}_j = [\hat{x}_j(0), \hat{x}_j(1), ..., \hat{x}_j(N_s-1)]^T$, j=0~J–1 as

$$\begin{aligned} \hat{\mathbf{x}}_j &= \mathbf{F}^H_{N_s} \hat{\mathbf{X}}_j \\ &\approx \sqrt{\frac{2E_s}{T_s}} \mathbf{F}^H_{N_s} \left(\left(\sum_{n_r=0}^{N_r-1} \sum_{n_t=0}^{N_t-1} \mathbf{H}_{n_r,n_t} \mathbf{W}_{n_r,n_t} \mathbf{W}^H_{n_r,n_t} \mathbf{H}^H_{n_r,n_t} \right) \mathbf{X}_j \right). \end{aligned} \qquad (11)$$

It is seen that the summation term in front of $\mathbf{X}_j$ is the diversity gain. Note that there still exists the phase rotation regarding to SLM in $\hat{\mathbf{x}}_j$.

3.2. 2-step phase rotation sequence estimation

In general, the received symbol vector $\hat{\mathbf{d}} = [\hat{\mathbf{d}}_0, \hat{\mathbf{d}}_1, ..., \hat{\mathbf{d}}_{J-1}]^T$, j=0~J–1 is obtained by employing de-mapping, i.e. multiplying $\hat{\mathbf{x}}_j$ by $\mathbf{P}^H_{\tilde{m}_j}$, but it requires side-information transmission. We have introduced an ML estimation for estimating the phase rotation sequence $\mathbf{P}_{\tilde{m}_j}$ [7-8], which its index $\tilde{m}_j$ can be expressed by

$$\tilde{m}_j = \arg \min_{\substack{m=0,1,...,M-1, \\ \mathbf{d}\in\Psi_{\text{mod}}}} \left(\varepsilon = \left\| \mathbf{P}^H_m \hat{\mathbf{x}}_j - \mathbf{d} \right\|^2 \right), \qquad (12)$$

where $\|\cdot\|$ represents the Euclidean norm and Ψ_{mod} is the original data-modulated constellation. Note that $\mathbf{d}$ is not considered as an output in this paper. However, eq. (12) requires very high complexity when M is large. In this paper, we alternatively introduce 2-step estimation, in which the first step initially searches the phase rotation sequence by using Viterbi algorithm. Verification and correction are employed in the second step. Hereinafter, the detection is applied to an individual block, hence the index j can be neglected for simplicity.

Step 1: Viterbi algorithm

The objective function ε in (12) can be rewritten by ignoring the codebook and assuming that Φ_{SLM} is a set of possible rotation patterns which is $\{1, e^{i2\pi/3}, e^{i4\pi/3}\}$ as

$$\arg \min_{\substack{\phi(t)\in\Phi_{SLM} \\ d\in\Psi_{\text{mod}}}} \left(\varepsilon = \sum_{t=0}^{N_s-1} \frac{1}{N_s} \left| \phi^*(t) \hat{x}_j(t) - d \right|^2 \right). \qquad (13)$$

Then, ε at time index t=T, 0<T≤N_s–1 is expressed by

$$\begin{aligned} \varepsilon(T) &= \sum_{t=0}^{T} \frac{1}{N_s} \min_{\substack{\phi(t)\in\Phi_{SLM} \\ d\in\Psi_{\text{mod}}}} \left| \phi^*(t) \hat{x}_j(t) - d \right|^2 \\ &= \varepsilon(T-1) + \frac{1}{N_s} \min_{\substack{\phi(t)\in\Phi_{SLM} \\ d\in\Psi_{\text{mod}}}} \left| \phi^*(T) \hat{x}_j(T) - d \right|^2. \end{aligned} \qquad (14)$$

We can search an optimal phase rotation sequence $\phi_{\text{opt}}(t)$, t=0~N_s–1 by using Viterbi algorithm. The first term and second term in (14) are considered as path metric at time t and state g, $\varepsilon(g_t)$, and branch metric from state g' at time t to state g at time t+1, $\zeta(g'_t \to g_{t+1})$, respectively, in the Viterbi algorithm. The trellis diagram assuming $G_{\max}$=3 states, i.e. g_t =0~2, is shown by Fig. 3.

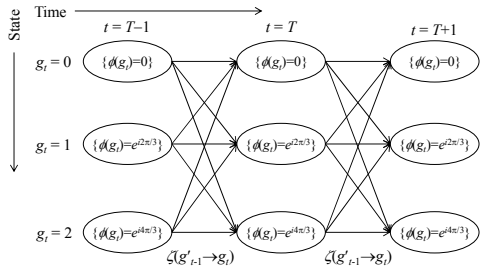

Fig. 3 Illustration of the trellis diagram with 3 states.

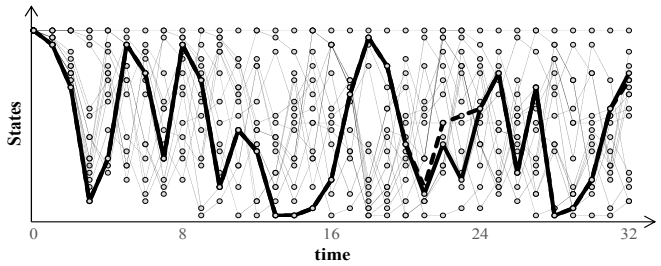

Fig. 4 An example of trellis diagram with reduced branches. (SC-FDE, 16QAM, N_c=32, M=16, Φ_{SLM}={1, $e^{i2\pi/3}$, $e^{i4\pi/3}$}, E_b/N_0 = 20 dB, solid path → correct path, dash path → output from Viterbi algorithm)

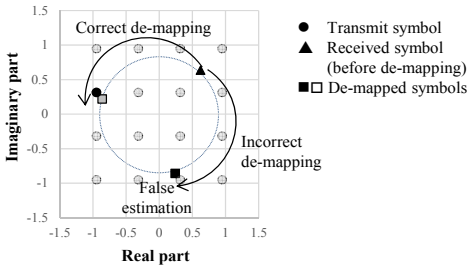

Fig. 5 Estimation error in Viterbi algorithm.

The initial path metric for each state at time t=−1 is set as $\varepsilon(g_{-1})$=0 for all g=0~$G_{\max}$−1. At a particular time index t where 0≤t≤N_s−1, the branch metric from state g' at time t to state g at time t+1 is expressed by

$$\zeta\left(g'_t \to g_{t+1}\right) = \frac{1}{N_s} \min_{d \in \Psi_{\text{mod}}} \left| \phi^*(g_{t+1}) \hat{x}_j(t+1) - d \right|^2, \tag{15}$$

where $\phi(g_{t+1})$ is the phase rotation at state g and time t+1. Then the path metric entering state g_{t+1} is selected by the following criterion.

$$\varepsilon(g_{t+1}) = \min_{g'_t=0,1,\ldots,G_{\max}} \left(\varepsilon(g'_t) + \zeta(g'_t \to g_{t+1}) \right). \tag{16}$$

Note that (15)-(16) are repeated until t=N_s−1. Once the path metric calculation is done until t=N_s−1, the surviving path metric which provides an optimal state number $g_{t,\text{opt}}$ and the optimal set of sequence $\phi_{\text{opt}}(t) = \phi(g_{t,\text{opt}})$, $t = 0,1,\ldots,N_s - 1$ can be determined by backward computation as follows.

$$g_{N_s-1,\text{opt}} = \arg \min_{g_{N_s-1,}=0,1,\ldots,G_{\max}} \varepsilon(g_{N_s-1,}), \tag{17a}$$

$$g_{t',\text{opt}} = \arg \min_{g_{t'}=0,1,\ldots,G_{\max}} \left(\varepsilon(g_{t'}) + \zeta(g_{t'} \to g_{t+1,\text{opt}}) \right),$$
where $t' = N_s - 2, N_s - 3, \ldots, 0.$ (17b)

We assume $G_{\max}$=27 in this paper, meaning that the phase rotation patterns in a particular state g_t is determined as a set $\{\phi(g_t;t-2), \phi(g_t;t-1), \phi(g_t;t)\}$. An increasing of $G_{\max}$ leads to an increasing of branches, where the redundant branches and states (i.e. the branches and states which do not exist in the codebook) can be removed prior to estimation. This can improve the accuracy of estimation and simultaneously reduce the complexity. Fig. 4 shows an example of 27-state trellis with N_s=32 and M=16, where we can observe that the redundant branches and states are removed.

However, the estimated phase rotation sequence from Viterbi algorithm $\phi_{\text{opt}}(t)$, t=0~N_s−1 still has error due to frequency-selective fading and noise. This is also shown in Fig. 4 and assuming the average received bit energy-per-noise power spectrum density (E_b/N_0) equals 20 dB that the selected path (dash line) is different from the actual phase rotation sequence used at the transmitter (bold solid line). The cause of error can be described by referring Fig. 5, which shows the received signal and the de-mapped signals at t=22. It is seen that the received symbol with incorrect de-mapping gives lower Euclidean distance from original constellations than that of correct de-mapping. The Viterbi algorithm is aiming at selecting the path with the lowest MSE, hence the incorrect sequence is selected as a surviving path instead. A possible solution for solving the above problem is phase rotation sequences design since we assume that the set of sequences is randomly generated. The topic of phase sequences design is left as our future works. Alternatively, we introduce verification and correction as the second step for reducing the error occurred in Viterbi decoding.

Step 2: Verification & correction

It is observed from Fig. 4 that the estimated phase sequence obtained from Viterbi decoding contains errors on few samples only when the received E_b/N_0 is sufficiently high. These errors can be corrected by checking the similarity of output from Viterbi decoding and the available phase rotation sequences in the codebook. Here, Hamming distance is used as an indicator for checking the similarity since the difference in rotation angle does not affect the data detection error. The phase rotation sequence in the codebook having the minimum Hamming distance from the output of Viterbi decoding is chosen. This approach confirms that the estimated phase sequence obtained from 2-step estimation is always available in the codebook.

Let $\mathbf{\Phi}_{\text{opt}} = diag[\phi_{\text{opt}}(0), \phi_{\text{opt}}(1), \ldots, \phi_{\text{opt}}(N_s-1)]$ denote the phase rotation sequence matrix obtained from the Viterbi decoding. The estimated phase rotation sequence for de-mapping $\mathbf{P}_{\tilde{m}} = diag[P_{\tilde{m}}(0), P_{\tilde{m}}(1), \ldots, P_{\tilde{m}}(N_s-1)]$ can be determined by

$$\mathbf{P}_{\tilde{m}} = \arg \min_{\mathbf{P}_m, m=0,1,\ldots,M-1} d\left(\mathbf{\Phi}_{\text{opt}}, \mathbf{P}_m\right), \tag{18}$$

Table 2 Simulation parameters.

Transmitter	Data modulation	16QAM
	FFT/IFFT points	N_c = 256
	No. of symbols per block	N_s = 64, 256
	CP length	N_g = 16
	Phase sequence type	Random polyphase
Channel	Fading	Frequency-selective block Rayleigh
	Power delay profile	Symbol-spaced, 16-path uniform
Receiver	Channel estimation	Ideal
	FDE	MMSE

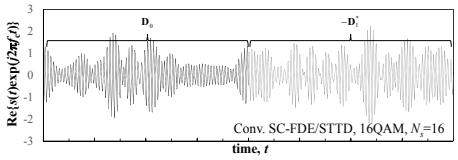

(a) Conventional SC-FDE/STTD

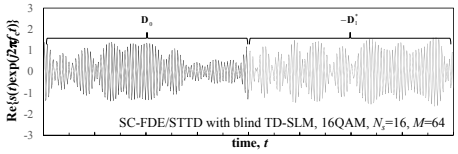

(b) SC-FDE/STTD with blind SLM

Fig. 6 Transmit waveforms.

where $\mathbf{P}_m = diag[P_m(0), P_m(1), ..., P_m(N_s-1)]$ is the m-th phase rotation sequence in the codebook and $d(\mathbf{A},\mathbf{B})$ represents the Hamming distance between matrices $\mathbf{A}$ and $\mathbf{B}$. Finally, the de-mapped symbols vector is obtained by $\hat{\mathbf{d}} = \mathbf{P}_{\hat{m}}^{H}\hat{\mathbf{x}}$.

4. Performance Evaluation

Numerical and simulation parameters are summarized in Table 2. Channel coding is not considered. A set of phase rotation sequences is generated in random approach from polyphase rotations $\{e^{j0}, e^{i2\pi/3}, e^{i4\pi/3}\}$ which are not optimal but sufficient for allowing blind TD-SLM [6].

4.1. Transmit waveforms

Figs. 6(a) and 6(b) show one-shot observation of 16QAM-modulated transmit waveforms of SC-FDE/STTD and SC-FDE/STTD using blind SLM at the transmit antenna #0, assuming N_t=2, N_s=16 and M=64. CP insertion is neglected for simplicity. The high peak is observed in Fig. 6(a) where there is no high peak in Fig. 6(b). This is consistent with [8] where the blind TD-SLM can reduce the PAPR up to 2.6 dB when M=64 even in multi-antenna transmission. Applying the phase rotation to the data-modulated symbols leads to phase shift on the filter impulse response, which can avoid peak amplitude occurred by the overlapping of pulses.

4.2. BER performance

Figs. 7(a) and 7(b) show the BER performances of SC-FDE/STTD using blind TD-SLM as a function of average received E_b/N_0 per antenna where $E_b/N_0=(1/N_{\text{mod}})(E_s/N_0)(1+N_g/N_c)$ with N_{mod} represents modulation level (4 for 16QAM). The number of transmit and receive antennas for STTD (N_t,N_r) is assumed to be (1,1) and (2,4). BER of conventional SC-FDE/STTD is also provided for comparison. The number of phase rotation sequence is set to be M=512.

Firstly, it is seen that the BER of phase rotation sequence estimation using only Viterbi decoding is the worst. It is observed that the BER improves when (N_t,N_r) increases due to higher spatial diversity gain [2]. When N_s=64, BER performances of both blind SLM using ML estimation and 2-step estimation degrade since the frequency-selective fading decreases the received signal power. However, both ML and 2-step estimations achieve similar BER performance compared to the conventional SC-FDE/STTD when (N_t,N_r)=(2,4). This is because the STTD combined with MMSE-FDE can effectively mitigate the spectrum distortion occurred in the received signal and accordingly improving the accuracy of phase rotation sequence estimation. It is also observed that there is no significant BER degradation even though there is no STTD when N_s=256, since higher frequency diversity gain can be obtained compared to the case of N_s=64.

The 2-step estimation achieves worse BER than ML estimation when E_b/N_0 is low. This is because the noise power makes the estimation error in Viterbi algorithm become more severe, and consequently verification and correction cannot find the correct phase rotation sequence from the codebook. Meanwhile, there is no significant BER degradation in 2-step estimation when E_b/N_0 is sufficiently high. This concludes that the 2-step estimation can be used for blind TD-SLM, while its complexity is expected to be much lower than ML estimation. Computational complexity is evaluated in the next subsection.

Table 3 Computational complexity.

	No. of real-valued multiplications	No. of real-valued additions
ML estimation	$M \times \left(N_s \times \left(4 + 2N_{\text{mod}}^2\right) + 1\right)$	$M \times N_s \times \left(3 + 3N_{\text{mod}}^2\right)$
2-step estimation	$N_{\text{trellis}} \times \left(6 + 2N_{\text{mod}}^2\right)$	$\left(N_{\text{trellis}} \times \left(3 + 3N_{\text{mod}}^2\right)\right) + (M \times N_s)$

4.3. $PAPR_{0.1\%}$ vs computational complexity

Computational complexity is defined by counting the number of real-valued multiplication and real-valued addition operations. Table 3 shows the computational complexity of ML estimation and 2-step estimation. It is seen from Table 3 that the complexity of ML estimation is a function of M. On the other hand, computational complexity of 2-step estimation is almost independent from M and is an order of N_{trellis}, where N_{trellis} is always less than or equal to $(81\times(N_s-2))+27$ if $G_{\max}$=27.

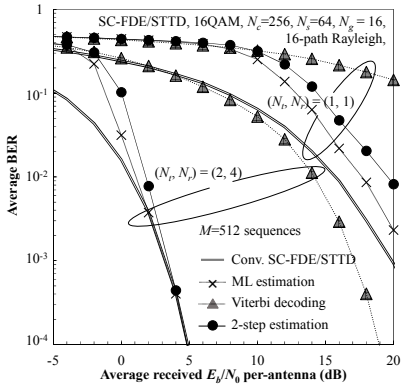

(a) N_s=64

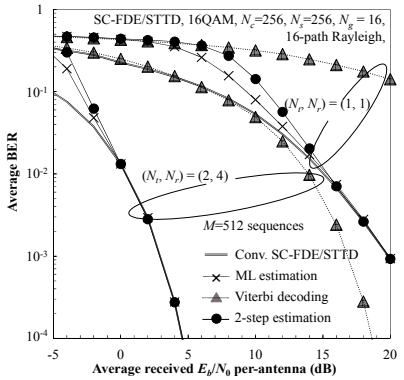

(b) N_s=256

Fig. 7 BER performances.

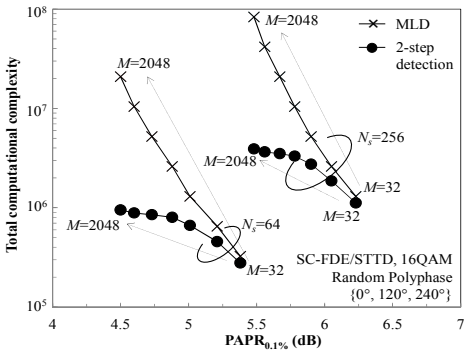

Fig. 8 $PAPR_{0.1\%}$ versus computational complexity.

Fig. 8 shows the $PAPR_{0.1\%}$ versus total computational complexity. $PAPR_{0.1\%}$ is defined as the PAPR value at the complementary cumulative distribution function (CCDF) equals 10^{-3}, while the $PAPR_{0.1\%}$ of conventional SC-FDE/STTD are 8.4 dB when N_s=64 and 8.8 dB when N_s=256, respectively. Note that the PAPR is irrespective to N_t if the phase rotation sequence is selected individually at the j-th block [8]. Total computational complexity is defined by estimating the complexity of a real-valued multiplication operation is 3 times of real-valued addition, then counting the total number of real-valued addition [11]. It is seen that PAPR can be reduced when M increases. The complexity of ML estimation drastically increases when M increases. On the other hand, the complexity of 2-step estimation is much lower than that of the ML estimation when M≥128. For example, when M=512 and N_s=256, SC-FDE/STTD using blind SLM and 2-step detection achieves the PAPR of 5.6 dB (i.e., PAPR reduction of 3.2 dB) without significant BER degradation (see Fig. 6(b)), where the complexity is only 16.8% of the ML estimation. Therefore, 2-step estimation can achieve very low-PAPR signal by using large M without causing high-complexity problem at the receiver.

5. Conclusion

2-step phase rotation sequence estimation scheme for blind TD-SLM was proposed. The proposed 2-step estimation employs Viterbi algorithm and then, carries out verification and correction for improving estimation accuracy. Computer simulation results confirmed that the 2-step estimation achieves similar BER performance compared to the ML estimation although its computational complexity is much lower. As a consequence, we can increase the number of phase rotation sequences for further lowering the PAPR.

Acknowledgement

This paper includes a part of results of "The research and development project for realization of the fifth-generation mobile communications system" (#0155-0019, April 2016) commissioned to Tohoku University by The Ministry of Internal Affairs and Communications (MIC), Japan.

References

[1] D. Falconer, S. L. Ariyavisitakul, A. Benyamin-Seeyar and B. Edison, "Frequency Domain Equalization for Single-Carrier Broadband Wireless Systems," *IEEE Commun. Mag.*, Vol. 40, No. 4, pp. 58-66, Apr. 2002.

[2] S. M. Alamouti, "A simple transmit diversity technique for wireless communications," *IEEE J. Select. Areas. Commun.*, Vol. 16, No. 8, pp. 1451-1458, Oct. 1998.

[3] K. Takeda, T. Itagaki and F. Adachi, "Application of Space-Time Transmit Diversity to Single-Carrier Transmission with Frequency-Domain Equalization and Receive Antenna diversity in a Frequency-Selective Fading Channel," *IEE Proc.-Commun.*, Vol. 151, No.6, pp. 627-632, Dec. 2004.

[4] H. G. Myung, J. Lim and D. J. Goodman, "Single Carrier FDMA for Uplink Wireless Transmission," *IEEE Veh. Technol. Mag.*, Vol. 1, No. 3, pp. 30-38, Sept. 2006.

[5] A. Boonkajay, T. Obara, T. Yamamoto and F. Adachi, "Excess-Bandwidth Transmit Filtering Based on Minimization of Variance of Instantaneous Transmit Power for Low-PAPR SC-FDE," *IEICE Trans. Commun.*, Vol. E98-B, No. 4, pp. 673-685, Apr. 2015.

[6] A. Boonkajay and F. Adachi, "Selected Mapping Technique for Reducing PAPR of Single-Carrier Signals," *Wireless Commun. And Mobile Computing*, Jun. 2016.

[7] A. Boonkajay and F. Adachi, "A Blind Polyphase Time-Domain Selected Mapping for Filtered Single-Carrier Signal Transmission," *in Proc. IEEE Veh. Technol. Conference* (VTC2016-Fall), Montréal, Canada, Sept. 2016.

[8] A. Boonkajay and F. Adachi, "Blind Selected mapping Techniques for Space-Time Block Coded Filtered Single-Carrier Signals," *in Proc. IEEE VTS Asia Pacific Wireless Commun. Symp. (APWCS2016)*, Tokyo, Japan, Aug. 2016.

[9] A. Viterbi, "Error Bound for Convolutional Codes and an Asymptotically Optimum Decoding Algorithm," *IEEE Trans. Inform. Theory*, Vol. 13, No. 2, pp. 260-269, Apr. 1967.

[10] G. Ganesan and P. Stoica, "Space-time block codes: A maximum SNR approach," *IEEE Trans. Inform. Theory*, Vol. 48, No. 2, pp. 1650–1656, Apr. 2001.

[11] S. Arora and B. Barak, *Computational Complexity: A Modern Approach*, Cambridge, 2009.